ISSN 0915-633X

NATIONAL INSTITUTE FOR FUSION SCIENCE

Transition in Multiple-scale lengths Turbulence in Plasmas

S.-I. Itoh, K. Itoh, M. Yagi, M. Kawasaki and A. Kitazawa

(Received - Jan. 31, 2002)

NIFS-725 Feb. 2002

RESEARCH REPORT
NIFS Series

TOKI, JAPAN

Transition in multiple-scale-lengths turbulence in plasmas

S.-I. Itoh[a], K. Itoh[b], M. Yagi[a], M. Kawasaki[a], A. Kitazawa[a]

[a] Research Institute for Applied Mechanics, Kyushu University, Kasuga 816-8580, Japan
[b]National Institute for Fusion Science, Toki, 509-5292, Japan

Abstract

The statistical theory of strong turbulence in inhomogeneous plasmas is developed for the cases where fluctuations with different scale-lengths coexist. Statistical nonlinear interactions between semi-micro and micro modes are first kept in the analysis as the drag, noise and drive. The nonlinear dynamics determines both the fluctuation levels and the cross field turbulent transport for the fixed global parameters. A quenching or suppressing effect is induced by their nonlinear interplay, even if both modes are unstable when analyzed independently. Influence of the inhomogeneous global radial electric field is discussed. A new insight is given for the physics of internal transport barrier. The thermal fluctuation of the scale length of λ_D is assumed to be statistically independent. The hierarchical structure is constructed according to the scale lengths. Transitions in turbulence are found and phase diagrams with cusp type catastrophe are obtained. Dynamics is followed. Statistical properties of the subcritical excitation are discussed. The probability density function (PDF) and transition probability are obtained. Power-laws are obtained in the PDF as well as in the transition probability. Generalization for the case where turbulence is composed of three-classes of modes is also developed. A new catastrophe of turbulent states is obtained.

Keywords:

statistical theory, strong turbulence, renormalization, multiple scale lengths, bifurcation, cusp catastrophe, butterfly catastrophe, subcritical excitation, probability density function, transition probability

I. INTRODUCTION

Recently, noticeable progress has been made in the field of theory and modelling of plasma turbulence. The development of a statistical theory for the strongly turbulent plasma has been one of the main subjects of plasma physics theory. Methodologies of turbulence theories has been advanced, and the theory for turbulence suppression and transition is a successful example for it. (See, for a review, e.g. refs.1-4.)

Fluctuations with different scale lengths coexist in plasmas. In a conventional approach, the scale separation is used, and one class of mode is analyzed where fluctuations of the other scale lengths are often neglected. This simplification is not always relevant. The importance of interactions between the modes with different scale lengths has recently been recognized. For instance, the dynamics of the meso-scale structure of the radial electric field[5] is known to cause varieties in the dynamics of microscopic fluctuations. Examples include the electric field domain interface,[6,7] zonal flow[8] and streamer,[9] and an effort to develop a statistical theory for zonal flow is reported.[10] It is shown that the mutual interactions between fluctuations with different scale lengths substantially influence the turbulence level.

In this paper, we analyze the turbulence composed of collective modes with different scale lengths. The nonlinear interplay and transition among them, phase diagram and statistical properties are analyzed. A new insight is given for the physics of internal transport barrier. The probability density function (PDF) of fluctuations, and the transition probability are presented. The fluctuation with two typical scale lengths is discussed first. The case with three scale lengths is also discussed and a new phase diagram is shown.

Hereafter we call the collective drift-type fluctuations the 'semi-micro mode' ($\sim \rho_i$) and distinguish it from the 'micro mode' of the scale of the skin depth ($\sim c/\omega_p$). Namely, $\rho_i > c/\omega_p$ holds in the system of our concern. The micro-turbulence is considered to cause the anomalous electron transport. The statistical nonlinear interplay (nonlinear dynamics) determines both the fluctuation levels and the cross-field turbulent transport. The term 'global' is used for the gradient scale lengths of the order of plasma radius a and the global parameters (averaged on magnetic surfaces) are given and fixed here. Thermal fluctuations of the order of the Debye length, λ_D, are assumed to be statistically independent of the modes of our concern.

The constitution of this paper is the following. In section II, the model and basic equations are given. Using a reduced set of equations for fluctuating fields, the self and mutual nonlinear interactions are formally divided into drags, drives and noises.[11-13] Then the Langevin equations are reformulated for each collective mode by introducing the scale separation. Statistical approach and the correlation functions (fluctuation level, transport quantities) in ref.14 is surveyed. An analysis based on the coarse grained quantity is given in section III, and explicit formulae are given for the interplay between

the current–diffusive interchange mode (CDIM)[1] of micro-turbulence and the ITG mode[3] of drift wave type semi-micro-turbulence. Possible nonlinear interactions and an insight for ITB are discussed. In section IV, the statistical properties are investigated by considering the nonlinear noise of turbulence and thermodynamical noise. The PDF and transition probability are analyzed. The case where fluctuations of three different scale lengths are interacting each other is analyzed in section V. The summary and discussion are given in section VI.

II. MODEL

A. Model equations and approximations

The derivation of statistical equation, which has been developed in previous articles, is briefly surveyed. The dynamical equations of fluctuation fields are given as

$$\frac{\partial}{\partial t} f + \mathcal{L}^{(0)} f = \mathcal{N}(f, f) + \tilde{S}_{th} \tag{1}$$

where $f^{\mathrm{T}} = \left(\phi, J_{\|}, V_{\|}, P_e, p_i\right)$ is the fluctuating component of electrostatic potential, parallel current, parallel velocity, electron pressure and ion pressure, and $\mathcal{N}(f, f)$ stands for the nonlinear terms $\mathcal{N}(f, f) = -\left(\nabla_{\perp}^{-2}\left[\phi, \nabla_{\perp}^2\phi\right], \left(1 - \xi\nabla_{\perp}^{-2}\right)^{-1}\left[\phi, J_{\|}\right], \left[\phi, V_{\|}\right], \left[\phi, P_e\right], \left[\phi, p_i\right]\right)$. The bracket $[f,g]$ denotes the Poisson bracket, $[f, g] = (\nabla f \times \nabla g)\cdot \boldsymbol{b}$, $\boldsymbol{b} = \boldsymbol{B}_O/B_O$ denotes the unit vector in the direction of the magnetic field and $\xi = \rho_i^2\delta^{-2}$. Physics variables (e.g., $\left\{\phi, A_{\|}, V_{\|}, p_e, p_i\right\}$, magnetic field B, electric field, length and time) are normalized according to a standard convention. Various choices of normalization are described in detail in ref.15. Transport coefficients by the collisional process are expressed by $\mu_{\perp c}$, $\mu_{e,c}$, $\mu_{\|c}$, $\chi_{c,e}$, $\chi_{c,i}$ for the shear viscosity, electron viscosity, parallel viscosity of ions, electron thermal diffusivity and ion thermal diffusivity, respectively.

In calculating the nonlinear drag term, fluctuations which have shorter wave-lengths are renormalized. The nonlinear terms are expressed as a sum of the drag, drive and the noise and are separated into semi-micro and micro modes, as

$$\mathcal{N}^l(f, f) = -\left(\Gamma_{(l)}^l + \Gamma_{(h)}^l\right) f^l + \tilde{S}_{(l)}^l + \tilde{S}_{(h)}^l \tag{2a}$$

and

$$\mathcal{N}^h(f, f) = -\Gamma_{(h)}^h f^h + \mathcal{D}_{(l)}^h f^h + \tilde{S}_{(h)}^h, \tag{2b}$$

The superscripts l and h denote the semi-micro and micro modes, respectively, and the subscripts (l) and (h) denote the contributions from semi-micro and micro modes, respectively.

By use of Eqs.(2a) and (2b), Langevin equations are derived as

$$\frac{\partial}{\partial t}\boldsymbol{f}^{l}+\left(\boldsymbol{\mathcal{L}}^{(0)}+\boldsymbol{\Gamma}^{l}_{(l)}+\boldsymbol{\Gamma}^{l}_{(h)}\right)\boldsymbol{f}^{l}=\tilde{\boldsymbol{S}}^{l}_{(l)}+\tilde{\boldsymbol{S}}^{l}_{(h)}+\tilde{\boldsymbol{S}}_{th}\ , \quad \text{(semi-micro mode)} \quad (3)$$

and

$$\frac{\partial}{\partial t}\boldsymbol{f}^{h}+\left(\boldsymbol{\mathcal{L}}^{(0)}+\boldsymbol{\Gamma}^{h}_{(h)}-\boldsymbol{\mathcal{D}}^{h}_{(l)}\right)\boldsymbol{f}^{h}=\tilde{\boldsymbol{S}}^{h}_{(h)}+\tilde{\boldsymbol{S}}_{th}\ . \quad \text{(micro mode)} \quad (4)$$

The renormalized drag (coherent part) is given in a form of the eddy-viscosity type nonlinear transfer rate γ_j. A random-noise part is regarded to have a shorter decorrelation time than γ_j^{-1} according to rapid change model.[11, 16] The nonlinear drag term is written in an apparent linear term as

$$\left(\boldsymbol{\Gamma}\boldsymbol{f}\right)^{\mathrm{T}}=-\left(\gamma_1 f_1,\ \gamma_2 f_2,\ \gamma_3 f_3,\ \gamma_4 f_4,\ \gamma_5 f_5\right)\ . \quad (5)$$

The driving part in the nonlinear interactions is deduced, giving $\mathcal{D}^{h}_{(l)\,j,\,j}=-i\,\omega_{E(l)}$ $(j=1\ ,\ j=3-5\ )$, $\mathcal{D}^{h}_{(l)\,2,\,2}=-i\,\xi^{-1}\omega_{E(l)}$, $\mathcal{D}^{h}_{(l)\,j,\,1}=-i\,\omega_{j(l)}$ $(j=3-5\ )$ and $\mathcal{D}^{h}_{(l)\,2,\,1}=-i\,\xi^{-1}\,\omega_{2(l)}$, where $\omega_{E(l)}=k_y\frac{\partial}{\partial x}\tilde{\phi}^{l}-k_x\frac{\partial}{\partial y}\tilde{\phi}^{l}$ is the Doppler shift owing to the $E\times B$ velocity associated with the semi-micro mode, and $\omega_{j(l)}=-k_y\frac{\partial}{\partial x}\tilde{f}^{l}_{j}+k_x\frac{\partial}{\partial y}\tilde{f}^{l}_{j}$ $(j=2-5\ )$ represents the modification of plasma parameter by the semi-micro mode.

B. Analysis of nonlinear statistical equations

1. Nonlinear Dispersion

Equations (3) and (4) might give a large amplitude solution where the operator in the left hand side vanishes. This provides a nonlinear dispersion relation, in which the effects of renormalized drag terms are included. The nonlinear dispersion relations are given as

$$\det\left(\lambda^{l}\boldsymbol{I}+\boldsymbol{\mathcal{L}}^{(0)}+\boldsymbol{\Gamma}^{l}_{(l)}+\boldsymbol{\Gamma}^{l}_{(h)}\right)=0\ , \quad (6a)$$

and

$$\det\left(\lambda^{h}\boldsymbol{I}+\boldsymbol{\mathcal{L}}^{(0)}+\boldsymbol{\Gamma}^{h}_{(h)}-\boldsymbol{\mathcal{D}}^{h}_{(l)}\right)=0\ , \quad (6b)$$

where λ^l and λ^h are nonlinear eigenvalues for the semi-micro mode and micro mode, respectively.

2. Statistical approach

In the turbulent state the contribution of the nonlinear noise is considerably large, and is not always negligibly small. From the solution of the Langevin equations (3) and (4), a statistical average of fluctuation amplitude is derived. The Fluctuation Dissipation (FD) relation, that the average of fluctuation amplitude and noise satisfy, has been derived. After a statistical average, the decorrelation rate agrees with the eigenvalue λ.

With the help of diagonalization approximation, by which the correlation function of noise terms are represented by the autocorrelation of fluctuations, [12, 13] one has an explicit form of the FD relation. The eddy-damping rate γ_j is related to the fluctuation amplitude through renormalization relation. Equation (6), the FD relation and the renormalization relation for eddy damping rate form a closed set of equations that determines the fluctuation level $I^{l,h}$, the decorrelation rate $\lambda^{l,h}$ and the eddy-damping rate $\gamma_v^{l,h}$ simultaneously in the presence of global inhomogeneities.

3. PDF and transition probability

Form the Langevin equations (3) and (4), the Fokker-Planck equations are deduced, and the probability density functions (PDF) can be obtained. If multiple solutions are allowed for a given set of parameters, it is called *hysteresis*. In the presence of statistical noise, a probabilistic transition between different branches of hysteresis takes place. The transition probability can be obtained by use of the PDF.

III. NONLINEAR INTERPLAY AND TRANSITION IN MULTIPLE-SCALE-LENGTHS TURBULENCE

A. Nonlinear interactions

The effect of the semi-micro mode to the micro mode is taken as follows: the local pressure steepening and the stretching the micro vortex. The former has the destabilizing influence and the latter has suppressing effect. The change of local magnetic shear by the semi-micro mode might be influential. However, this effect is not kept here, and is left for future study.

Combining Eq. (6), the FD relation and renormalization relation for eddy damping rate, we have a set of nonlinear equations for the spectral intensities of the semi-micro mode $I^l = \sum_k \left\langle f_{1,k}^{l\,*} f_{1,k}^{l} \right\rangle$ and micro mode $I^h = \sum_k \left\langle f_{1,k}^{h\,*} f_{1,k}^{h} \right\rangle$ as[14]

$$\left(\frac{\sqrt{I^h} + \sqrt{I^h + 4I^l}}{2} - D^l \right) I^l = \varepsilon \left(I^h \right)^{3/2} \qquad \text{(semi-micro mode)} \quad (7a)$$

and

$$I^h = \left(D^h\right)^2 \frac{1}{\left(1 + I_{eff}^{-1} I^l\right)^2} \left(1 + \frac{\sqrt{I^l}}{\sqrt{I^h} + \sqrt{I^h + 4I^l}}\right) . \quad \text{(micro mode)} \tag{7b}$$

In these equations, $\varepsilon = \hat{C}_0^h \left(2 - C_0^l\right)^{-1} \left(k_0^l / k_0^h\right)^2$ implies the noise source (pumping) from the micro mode to the semi-micro mode,

$$D^l = \frac{2}{2 - C_0^l} \frac{1}{k_0^{l\,2}} \frac{\gamma_0^l}{1 + \left(\omega_{E1} / \omega_{Ec}^l\right)^2} . \tag{8a}$$

and

$$D^h = \frac{2}{2 - C_0^h} \frac{1}{1 + \left(\omega_{E1} / \omega_{Ec}^h\right)^2} \frac{\gamma_0^h}{k_0^{h2}} , \tag{8b}$$

denote the driving source from inhomogeneities for the semi-micro mode and micro mode, C_0^l , C_0^h and $\hat{C}_0^h$ are numerical coefficients of the order of unity that show the contribution of nonlinear noise, and k_0^l and k_0^h are typical wavenumbers of the semi-micro and micro modes, respectively. The parameters D^l and D^h denote the magnitudes of the drives due to global inhomogeneity and are turbulent transport coefficient in the absence of mutual nonlinear interactions. In Eqs.(8a) and (8b), γ_0 stands for the each nonlinear growth rate without coupling and nonlinear noise, ω_{E1} is the $E \times B$ shearing rate by the global radial electric field,

$$\omega_{E1} = \frac{1}{B} \frac{d}{dr} E_r , \tag{9}$$

$\omega_{E\,c}^l$ and $\omega_{E\,c}^h$ are the critical values for the suppression of the modes. The parameter

$$I_{eff} \equiv \left(1 + \left(\omega_{E1} / \omega_{Ec}^h\right)^2\right) \left(\omega_{Ec}^h\right)^2 \left(k^l\right)^{-4} . \tag{10}$$

represents the amplitude of semi-micro mode above which the $E \times B$ shear stabilization is effective.

In the absence of the mutual nonlinear interactions, one has

$$I^l = \left(D^l\right)^2 \text{ and } I^h = \left(D^h\right)^2 . \tag{11}$$

which implies both the modes can be unstable and excited independently.

Combining equations (7a) and (7b), the self-consistent solution is obtained. This system is characterized by parameters D^l , D^h , I_{eff} and ε . This system of equations has three types of solutions; micro-mode dominant solution, semi-micro-mode dominant solution and bistable solutions. For the case of micro-mode dominant solution, the semi-micro mode is quenched

$$I^h \simeq \left(D^h\right)^2 \text{ and } I^l \simeq \varepsilon\, I^h \,. \tag{12}$$

For the case of semi-micro-mode dominant solution, the level of micro mode is suppressed as

$$I^h \simeq D^{h2}\, I_{eff}^2\, D^{l-4} \text{ and } I^l \simeq \left(D^l\right)^2 \,. \tag{13}$$

Figure 1 illustrates the phase diagram on the plane of global driving parameters, being represented by D^l and D^h . Symbols 'micro' and 'semi-micro' stand for the regions where solutions of Eqs.(12) and (13) are obtained, respectively. In the region denoted by 'both', bistable solutions are given: both solutions of Eqs.(12) and (13) are allowed simultaneously. A cusp type catastrophe is obtained, and transition between different branch of fluctuations occurs.

It should be noted that the excited amplitudes of fluctuations are strongly modified by the presence of other fluctuations. In Fig.1, both semi-micro and micro modes are

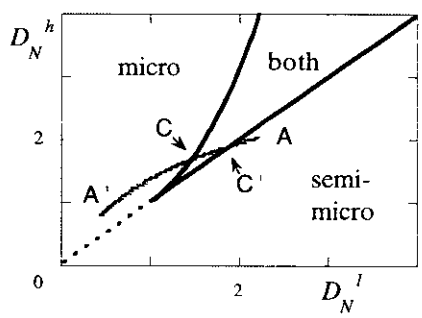

Fig.1 Phase diagram on the plane of global parameters, being represented by normalized driving parameters $D_N^h = D^h/\sqrt{I_{eff}^{h\leftarrow l}}$ and $D_N^l = D^l/\sqrt{I_{eff}^{h\leftarrow l}}$ ($\varepsilon = 0$). A cusp type catastrophe is obtained. In the region of "micro", the semi-micro mode level is quenched and is very low. In the region of "semi-micro", the micro mode coexists but is suppressed. Trajectory of the driving parameters $D^l\left(\omega_{E1}^l\right)$ and $D^h\left(\omega_{E1}^h\right)$ is shown by A-A' and B-B', as the global electric field shear increases. ω_{E1} changes from $\omega_{E1}/\omega_{Ec}^l = 0$ to $\omega_{E1}/\omega_{Ec}^l = 2$. On A-A', a hard transition takes place at C and the back-transition at C'. $D^l(0) = 2.2\sqrt{I_{eff}}$, $D^h(0) = 2\sqrt{I_{eff}}$ and $\omega_{Ec}^l = \sqrt{0.4}\ \omega_{Ec}^h$ for (A-A'); $D^l(0) = \sqrt{I_{eff}}$, $D^h(0) = 0.6\sqrt{I_{eff}}$ and $\omega_{Ec}^l = \sqrt{0.3}\ \omega_{Ec}^h$ for (B-B').

unstable everywhere. Nevertheless, the mutual interaction regulates the excited fluctuation levels. In a region of small D^l, the semi-micro mode is almost completely quenched. In the region of 'semi-micro', the semi-micro mode is dominantly excited; the micro mode is also excited but is suppressed by the nonlinear interplay.

The region 'semi-micro' and 'both' are given by the relations

$$D^l > D^h . \tag{14a}$$

and

$$D^l < D^h < \frac{1}{4\,D^l I_{eff}} \left(D^{l2} + I_{eff} \right)^2 . \tag{14b}$$

respectively.

B. Example of ITG and CDIM

The formalism is applied to a coupling between the ITG mode and the current-diffusive interchange mode (CDIM). We consider a system with the magnetic hill in the absence of the radial electric field shear. The ITG mode is chosen as a semi-micro mode, and the drive is given as[3]

$$D^l = 14 \left(\frac{T_i}{T_e} \right)^{3/2} \sqrt{\frac{R\left(1 - \eta_{ic} L_T / L_n\right)}{L_T}} \; \frac{c_s \rho_s^2}{R} \tag{15}$$

where the critical value η_{ic} is approximated here as $\eta_{ic} \simeq 1 + 2.5 L_n / R$. In this expression, L_T and L_n are the gradient scale lengths of the temperature and density, respectively, R is the majour radius, c_s is the ion sound speed and other notation is standard. The CDIM is chosen as a micro mode, and the drive is given as[5]

$$D^h = C \frac{G_0{}^{3/2}}{s^2} \frac{\delta^2}{\tau_{Ap}} \tag{16}$$

where G_0 is the normalized pressure gradient multiplied by the magnetic hill height, s is the magnetic shear, δ is the collisionless skin depth, τ_{Ap} is the poloidal-Alfven transit time qR / v_A, and C is a numerical coefficient of the order of unity. Both of driving parameters D^l and D^h have the dimensional dependence $T^{1.5} B^{-2} R^{-1}$. The competition between D^l and D^h takes place through the gradient scale lengths and a geometrical parameter. They are symbolically written as

$$D^l = A_{\mathrm{ITG}} \sqrt{\frac{R}{L_T} - \frac{R}{L_n} - 2.5} \quad \text{and} \quad D^h = A_{\mathrm{CDIM}} \left(\frac{R}{L_n} + \frac{R}{L_T} \right)^{3/2} \tag{17}$$

with $A_{\mathrm{ITG}} = 14\left(T_i/T_e\right)^{3/2} c_s \rho_s^2 / R$ and $A_{\mathrm{CDIM}} = C\left(\mathrm{hill}\cdot\beta\right)^{3/2} s^{-2}\delta^2 \tau_{Ap}^{-1}$. This system is controlled by the gradient parameters, R/L_n and R/L_T, together with the ratios $\sigma \equiv A_{\mathrm{CDIM}}/A_{\mathrm{ITG}} \propto A_i^{-1}\left(\mathrm{hill}\right)^{3/2} s^{-2}$ and $I_{\mathrm{eff}}/A_{\mathrm{ITG}}^2$. Figure 2 illustrates the phase diagram on the $(R/L_T\ ,\ R/L_n)$ plane. The ITG mode is dominantly excited if the temperature gradient exceeds the threshold value where the density gradient is weak. When the gradients become strong, the fluctuation is dominated by the CDIM. The L-mode plasmas in large toroidal confinement devices are considered to be in the regime of the "semi-micro".

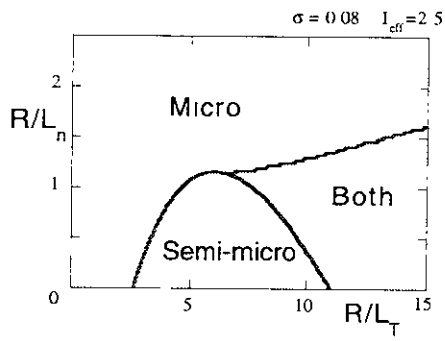

Fig. 2 Phase diagram on the plane of $(R/L_T\ ,\ R/L_n)$.

Figure 3 illustrates the fluctuation amplitude as a function of the temperature gradient with fixed density gradient. When the ion temperature gradient is low, the fluctuation is dominated by the CDIM. Once the ITG mode is excited, the CDIM is suppressed. By the presence of the CDIM, the threshold gradient of ITG mode is increased in comparison with the linear threshold. In the large gradient limit, the branch of CDIM (denoted by dotted line) appears again. With this branch, the ITG mode is a

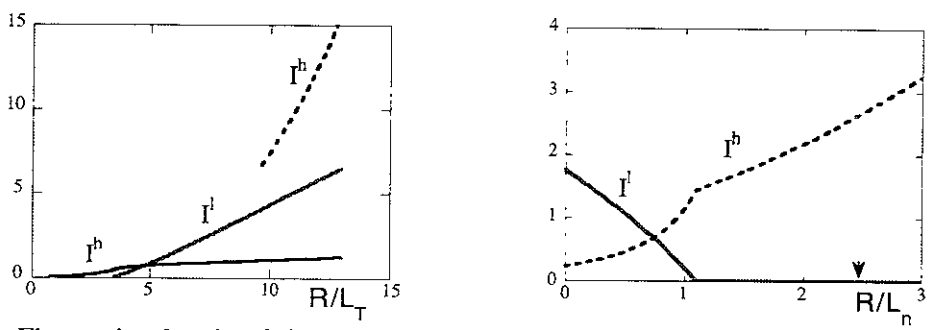

Fig.3 Fluctuation level. If the semi-micro mode is excited, the micro mode amplitude is shown by the solid line. Parameters are: (a) $R/L_n = 0.5$ and (b) $R/L_T = 5$. In (b), the arrow on the horizontal axis denotes the linear stability boundary. Other parameters are $I_{\mathrm{eff}}/A_{\mathrm{ITG}} = 2$, $\sigma = 0.08$, $\varepsilon = 0$.

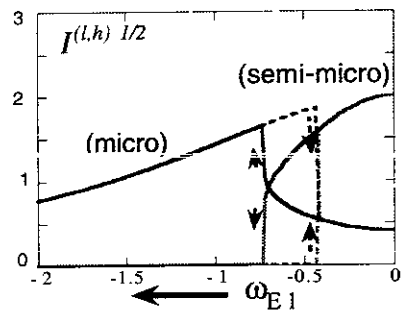

Fig.4 Fluctuation amplitudes $\sqrt{I^l}$ and $\sqrt{I^h}$ as a function of the shear of global $E \times B$ velocity $\omega_{E1}/\omega_{Ec}^l$. ω_{E1} changes from $\omega_{E1}/\omega_{Ec}^l = 0$ to $\omega_{E1}/\omega_{Ec}^l = 2$ along the line A-A' in Fig.1. ($\sqrt{I^l}$ and $\sqrt{I^h}$ are normalized to $\sqrt{I_{eff}}$.) Parameters are: $D^l(0) = 2.2\sqrt{I_{eff}}$, $D^h(0) = 2\sqrt{I_{eff}}$ and $\omega_{Ec}^l = \sqrt{0.4}\ \omega_{Ec}^h$. Hysteresis: solid curve for increasing $|\omega_{E1}|$ ($A \rightarrow A'$ in Fig.1) and dashed curve for decreasing $|\omega_{E1}|$ ($A' \rightarrow A$).

quenched solution. In the regime of the high temperature gradient, both the modes are possible to exist. Influence on the semi-micro mode is more explicitly seen in Fig.3(b). By the increment of the density gradient, a transition to the CDIM fluctuation occurs and the ITG mode is quenched. This transition takes place at much lower density gradient than the prediction of the linear stability of the ITG mode.

C. Implication to ITB formation

The nonlinear interplay introduces a new transition of fluctuations which gives an insight into an establishment of ITB. In usual circumstance, the effect of the electric field shearing rate for turbulence suppression is stronger for the semi-micro mode,

$$\omega_{Ec}^l < \omega_{Ec}^h . \tag{18}$$

If one considers the situation where the L-mode is in the region of "semi-micro" in the phase diagram (as is in Fig.2), then the trajectory of $D^l(\omega_E)$ and $D^h(\omega_E)$ on the phase diagram behaves like A-A' in Fig.1. Along this path, a transition is induced. On the path of A to C, the semi-micro mode is dominant. As the drive $D^l(\omega_E)$ is reduced by the electric field gradient, the semi-micro mode amplitude is decreased. In contrast, the amplitude of the micro mode increases. At the onset of transition to the micro mode solution, the semi-micro mode is quenched. Along the path C-A', the amplitude of the micro mode is suppressed by the increment of the electric field shear. When the electric field shear is reduced, as from A' to A in Fig.1, the transition to the semi-micro mode branch occurs at C'. Figure 4 shows the suppression and transition of turbulence by the

radial electric field shear. (The occurrence of transitions at C and C' is based on the deterministic picture of transition.)

Figure 5 illustrates a phase diagram for the case of Eq.(17). When the radial electric field shear increases, the transition to the micro mode takes place. The critical value of the electric field shear for quenching the semi-micro mode is strongly influenced by the coupling.

The induced transition of the semi-micro fluctuations sheds a light on the internal transport barrier (ITB) formation. A key problem in the ITB formation is the imbalance between the formations of ITBs for the ions and electrons.[17] In many cases, the electron thermal transport remains in the level of L-mode when the ITB for the ion energy is established. The ITB for electron thermal transport can also appear as the ITB for ion energy becomes prominent. This problem can be resolved by considering the mutual interactions between the semi-micro mode like ITG and the micro mode like ETG or CDBM turbulence. The response (solid curves) in Fig.4 illustrates that the semi-micro mode, which dominantly influences the ion transport, is reduced first; the micro mode that influences electron transport remains to be strong. The interchange between the semi-micro mode and micro mode takes place at the critical condition. These analysis might be compared to the experimental observations. In large tokamaks, both the fluctuations in the ranges of $k \leq \rho_i^{-1}$ and $k \sim c/\omega_p$ have been observed (e.g., in ref.18 and 19, respectively). When the ITB is formed the longer wavelength fluctuations are strongly quenched,[20] but shorter one remains at the moderate amplitude and relation with residual electron anomalous transport has been discussed.[18, 21] The current diffusive turbulence with correction of finite-ion-gyroradius-effect is analyzed in ref.22.

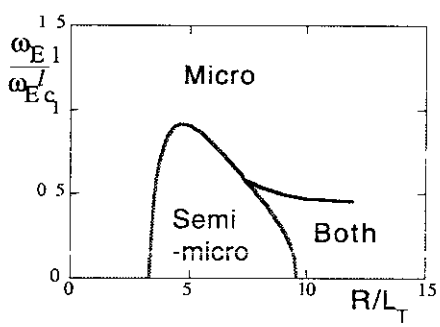

Fig.5 Example of turbulence transition for the case of $\omega_{Ec}^{l} = \sqrt{0.4}\ \omega_{Ec}^{h}$.

IV. STATISTICAL PROPERTIES AND TRANSITION DYNAMICS

The background turbulence causes on a test mode the nonlinear noise which gives rise to the statistical variation and the probabilistic transition. The statistical properties

and probabilistic transitions are discussed taking an example of the CDIM turbulence and thermodynamical fluctuations.

A. Statistical approaches

An average in a small volume of fluctuation energy $\mathcal{E} \equiv \frac{1}{2} \sum_{k < L^{-1}} k_\perp^2 \phi_k^2$ is introduced. (L denotes the size of region where the volume average is taken.) The Langevin equation for this single coarse-grained quantity is obtained from Eq.(2) as

$$\frac{\partial}{\partial t} \mathcal{E} + 2\Lambda \mathcal{E} = g\, \tilde{w}(t) \tag{19}$$

where the drag and noise terms are given as $\Lambda \equiv \mathcal{E}^{-1} \sum_k \lambda_{1,k} k_\perp^2 \phi_k^2$ and $g = \sum_k k_\perp^2 \tilde{s}_k \phi_k$, respectively. The coefficient Λ is the averaged decorrelation rate. A magnitude of the noise term is estimated as

$$g^2 = \sum_k 2\mu_{vc} \hat{T} k_\perp^4 \phi_k^2 + \sum_k \left(\sum_{j=1}^{3} A_{1j} g_{j,k} \right)^2 k_\perp^4 \phi_k^2 \tag{20}$$

where the first term in the RHS of Eq.(20) is the contribution from the thermal fluctuations and the second is the one from turbulent fluctuations. In Eq.(20), $\hat{T}$ is a normalized temperature, $\hat{T} = 2\mu_0 B_p^{-2} k_B T$, and $\boldsymbol{A}$ stands for the coefficient to $\exp\left(-\lambda_1 \tau\right)$ in the spectral decomposition of $\exp\left(-\mathcal{L}\tau\right)$ where $\mathcal{L}$ is the renormalized operator.[12]

The Fokker-Planck equation for the probability distribution function $P(\mathcal{E})$ is given as

$$\frac{\partial}{\partial t} P(\mathcal{E}) = \frac{\partial}{\partial \mathcal{E}} \left(2\Lambda \mathcal{E} + \frac{1}{2} g \frac{\partial}{\partial \mathcal{E}} g \right) P(\mathcal{E}) \tag{21}$$

The probability density function (PDF) is strongly influenced by the asymptotic behaviours of the damping rate Λ and the noise source g^2. From the renormalization relation, asymptotic estimates are given as

$$\Lambda = \bar{\bar{\Lambda}} \left(\frac{\mathcal{E}}{\mathcal{E}_{eq}} \right)^{1/2} \text{ and } g^2 = 4\hat{T}\gamma_m \mathcal{E} + \bar{\bar{g}}_0^2 \left(\frac{\mathcal{E}}{\mathcal{E}_{eq}} \right)^{5/2}, \tag{22}$$

where $\mathcal{E}_{eq}$ represents the statistical average of the fluctuation level. The coefficients $\bar{\bar{\Lambda}}$ and $\bar{\bar{g}}_0^2$ are given as $\bar{\bar{\Lambda}} = \lim_{\mathcal{E} \to \infty} \Lambda \left(\frac{\mathcal{E}}{\mathcal{E}_{eq}} \right)^{-1/2}$ and $\bar{\bar{g}}_0^2 \simeq \sum_k \left(\sum_{j=1} A_{1j} g_{j,k} \right)^2 k_\perp^4 \phi_k^2$ at $\mathcal{E} = \mathcal{E}_{eq}$.

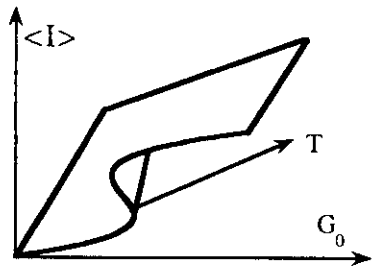

Fig.6 Schematic illustration of the statistical average of fluctuation level $\langle I \rangle$ as a function of the global gradient and temperature.

B. Thermodynamical and turbulent fluctuations

The subcritical excitation of the CDIM turbulence from thermal fluctuation has been analyzed in e.g., ref.5. The fluctuation level is described by the pressure gradient G_0 and the temperature $\hat{T}$. The former is the driving source of instability and the latter is the thermodynamical noise source. The cusp-type catastrophe has been obtained as is shown in Fig.6.

Parameter dependencies has been obtained as[13]

$$\mathcal{E}_{eq} = \frac{1}{4} G_0^2 \left(\frac{\delta}{s\,a}\right)^2 \left(\frac{L}{a}\right)^2 , \tag{23a}$$

$$\bar{\bar{\Lambda}} \simeq G_0^{1/2} \tag{23b}$$

and

$$\bar{\bar{g}}_0^2 \simeq \frac{C_0}{6} G_0^{11/2} \left(\frac{\delta}{s\,a}\right)^6 \left(\frac{L}{a}\right)^2 . \tag{23c}$$

The Langevin equation (19) is solved and the PDF is given in Fig.7. In the case

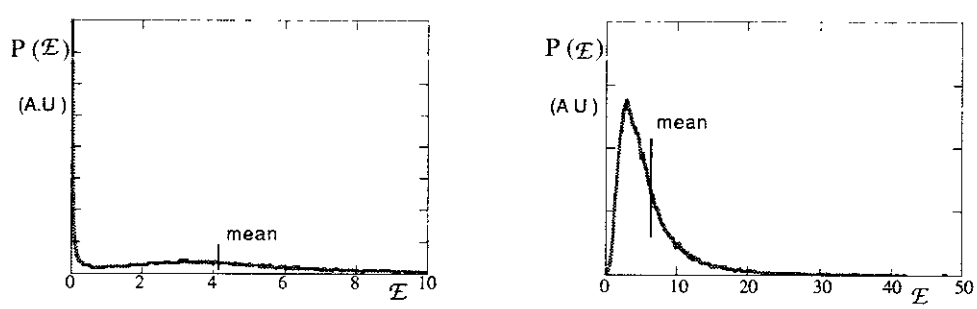

Fig. 7 PDF for the CDIM turbulence obtained from Langevin equation in the presence of the thermodynamical noise source. The case of hysteresis region is given in (a). The case of large pressure gradient is shown in (b).

of hysteresis region of Fig.6, in which two states (turbulent state and thermodynamical noise state) are possible, the fluctuation amplitude is either in the turbulent level or in the level of thermodynamical fluctuations.[23] Transition between the two states occurs very frequently, and the PDF of the long-time data shows a two peaks in $P(E)$. The tails of two peaks, i.e., the one for thermodynamical fluctuation and the one for turbulent fluctuation, overlap in Fig.7(a), allowing the transitions between them. The transition occurs in a probabilistic manner which is discussed later.

1. Probability density function (PDF)

The steady state PDF for the average energy P_{eq} is obtained by setting $\partial P/\partial t = 0$ in Eq.(21). It is expressed as

$$P_{eq}(\mathcal{E}) = \bar{P}\,\frac{1}{g}\exp\left(-S(\mathcal{E})\right) \tag{24a}$$

where

$$S(\mathcal{E}) \equiv \int_0^{\mathcal{E}} \frac{4\Lambda}{g^2}\,\mathcal{E}\mathrm{d}\mathcal{E} \tag{24b}$$

is the potential function of the normalized dissipations and $\bar{P}$ is a normalization constant. This potential $S(\mathcal{E})$ dictates the statistical properties of the thermodynamical and turbulent fluctuations. Equation (24a) shows that the most probable state is controlled by the condition $S(\mathcal{E}) + \ln g$ takes the minimum. This minimum principle is shown to reduce to the Prigogine's minimum-entropy-production-rate principle[24] or to the Boltzmann's maximum-entropy principle if one takes the limit of the thermodynamical equilibrium.

Substituting Eq.(22) into Eq.(24), one has an explicit formula of PDF for the system of CDIM turbulence and thermodynamical fluctuations. The analysis in the large amplitude limit has shown the existence of a tail component. One finds an asymptotic form in the large $\mathcal{E}$ limit as

$$P_{eq}(\mathcal{E}) \propto \left(\frac{\mathcal{E}}{\mathcal{E}_{eq}}\right)^{-\eta}, \tag{25}$$

with $\eta = 5/4 + 4\,\bar{\bar{\Lambda}}\,\bar{g}_0^{-2}\,\mathcal{E}_{eq}^2$. By use of Eq.(23), we have the relation for the power index as

$$\eta \simeq \frac{5}{4} + \frac{3}{2C_0}\,s\left(\frac{L}{\delta}\right)^2 G_0^{-1}. \tag{26}$$

This result shows that the power index depends on the gradient scale length as well as the size of volume average. As the pressure gradient becomes larger, the tail becomes prominent.[12]

2. *Transition probability*

The transition probability between two fluctuation states can be calculated by use of the potential $S(\mathcal{E})$. In the hysteresis region, $S(\mathcal{E})$ has two minima (at $\mathcal{E}=\mathcal{E}_A$ and $\mathcal{E}=\mathcal{E}_B$), separated by the maxima of $S(\mathcal{E})$ at $\mathcal{E}=\mathcal{E}_C$. (The state A stands for the thermodynamical fluctuations and B for turbulent fluctuations for the case of Fig.6.) The probabilities for the A-to-B and B-to-A transitions are given as[13]

$$r_{A\to B}=\frac{\sqrt{\Lambda_*\gamma_m}}{\sqrt{\pi}}\exp\left\{-S(\mathcal{E}_C)\right\} \tag{27a}$$

$$r_{B\to A}=\frac{\sqrt{\Lambda_*\gamma_B}}{4\sqrt{\pi}}\exp\left\{S(\mathcal{E}_B)-S(\mathcal{E}_C)\right\} \tag{27b}$$

where $\Lambda_*=-2\,\mathcal{E}\partial\Lambda/\partial E\Big|_C$ is estimated at the saddle point, γ_m is the average decorrelation rate of thermodynamical fluctuations and γ_B is the turbulent decorrelation rate at the state B. In the case of subcritical excitation from the thermodynamical fluctuations, Λ_* is estimated as $\Lambda_*\simeq\gamma_m$. In the thermodynamical limit of Eq.(27), one has $r_{A\to B}=\pi^{-1/2}\gamma_m\exp\left\{-\mathcal{E}_C/\hat{T}\right\}$. The dominant dependence is given as $\ln\left(r_{A\to B}\right)\propto -1/T$, which is the Arrhenius law.[25]

By use of the estimate of potential $S(\mathcal{E})$ in Eq.(25), transition probabilities are calculated. One has an estimate $\mathcal{E}_C$ for the typical wave number k_0 as $\mathcal{E}_C\simeq\left(\mu_{ec}^2/4\right)\left(k_0L\right)^2\left(1-G_0/G_c\right)$ in the vicinity of stability criterion G_c. The transition probability is evaluated as

$$r_{A\to B}\sim\frac{\gamma_m}{\sqrt{\pi}}\left(\frac{\mu_{ec}}{2}\right)^{-2b_1}k_0^{-4b_1/3}\left(\hat{T}\gamma_m\frac{3}{16C_0}\right)^{2b_1/3}\left(1-\frac{G_0}{G_c}\right)^{-b_1} \tag{28}$$

with the power-index as $b_1\simeq 3^{-1}\left(\left(3/16C_0\right)k_0\gamma_m\right)^{2/3}\hat{T}^{-1/3}\left(L/a\right)^2$. Explicit calculation will be given in ref.23.

V. THREE CLASSES OF FLUCTUATIONS AND THEIR INTERACTIONS

The analysis of transitions between two classes of turbulence can be extended to more general cases. The case of three classes of fluctuations are discussed here. We

assume that the scale length separation and time scale separation hold among them. Hereafter we treat the case without noises, $\tilde{S}=0$.

A set of equations which include the nonlinear interplay between three classes of fluctuations are expressed for fluctuation amplitudes I^m , I^l and I^h as

$$\frac{1}{4}\left(\sqrt{I^h}+\sqrt{I^h+4I^l}+\sqrt{\left(\sqrt{I^h}+\sqrt{I^h+4I^l}\right)^2+16I^m}\right)=D^m \quad (29a)$$

$$\frac{1}{2}\left(\sqrt{I^h}+\sqrt{I^h+4I^l}\right)=D^l\frac{\sqrt{1+\sqrt{I^m}/2D^m}}{\left(1+I^m I_{eff}^{lm-1}\right)} \quad (29b)$$

and

$$\frac{I^h}{\left(D^h\right)^2}=\frac{1+\sqrt{\dfrac{I_1^m}{4D^{m2}}+\dfrac{I_1^l}{4D^{l2}}\dfrac{\left(1+I^m I_{eff}^{lm-1}\right)^2}{\left(1+\sqrt{I^m}/2D^m\right)}}}{1+I_{eff}^{hl-1}I^l+I_{eff}^{hm-1}I^m} \quad (29c)$$

where the index m , l and h stands for the macro, semi-micro and micro mode fluctuations. In this set of equations

$$D^m=\left(1+\left(\omega_E/\omega_{Ec}^m\right)^2\right)^{-1}\gamma_0^m k_0^{m-2}, \quad (30a)$$

$$D^l=\left(1+\left(\omega_E/\omega_{Ec}^l\right)^2\right)^{-1}\gamma_0^l k_0^{l-2}, \quad (30b)$$

and

$$D^h=\left(1+\left(\omega_{E1}/\omega_{Ec}^h\right)^2\right)^{-1}\gamma_0^h k_0^{h-2} \quad (30c)$$

represent driving sources for the macro, semi-micro and micro mode fluctuations, and

$$I_{eff}^m\equiv\left(1+\left(\omega_E/\omega_{Ec}^l\right)^2\right)\left(\omega_{Ec}^l\right)^2\left(k^m\right)^{-4} \quad (31a)$$

$$I_{eff}^{hl}\equiv\left(1+\left(\omega_E/\omega_{Ec}^h\right)^2\right)\left(\omega_{Ec}^h\right)^2\left(k^l\right)^{-4} \quad (31b)$$

and

$$I_{eff}^{hm} \equiv \left(1 + \left(\omega_L/\omega_{Ec}^h\right)^2\right)\left(\omega_{Ec}^h\right)^2\left(k^m\right)^{-4} \qquad (31c)$$

stand for the characteristic fluctuation level at which the semi-micro mode is suppressed by the macro mode, the micro mode by the semi-micro mode and the micro mode by the macro mode, respectively. In the absence of the nonlinear interaction, three classes of fluctuations can be independently unstable and the levels are given by the solution

$$I^m \simeq \left(D^m\right)^2 , \; I^l \simeq \left(D^l\right)^2 \text{ and } I^h \simeq \left(D^h\right)^2 . \qquad (32)$$

Equation (29) is derived for the condition that all the three classes of fluctuations are excited. When one of them vanishes, the governing equation reduces to Eq.(7).

Solutions of Eq.(29) give a new catastrophe structure with multiple solutions. The driving parameters D^h , D^l and D^m are normalized to $\sqrt{I_{eff}^{h\leftarrow l}}$ which is the characteristic level of fluctuations for the semi-micro mode to suppress the micro mode. A phase diagram is drawn on the plane of normalized driving parameters $D_N^h = D^h/\sqrt{I_{eff}^{h\leftarrow l}}$ and $D_N^l = D^l/\sqrt{I_{eff}^{h\leftarrow l}}$ for the fixed value of $D^m = \left(1/5\right)\sqrt{I_{eff}^{h\leftarrow l}}$. The variation of the magnitude of drives changes the number of possible solutions. In the phase diagram of Fig.8, the regions for the number of possible solutions, where all three modes are simultaneously excited, are shown. In the region of strong drive for the semi-micro mode D^l , two, three and four branches of turbulent states are predicted to exist. When the drive for the micro mode D^h becomes strong, the micro mode dominates and the macro and the semi-micro modes are quenched. In the region denoted by "0", the simultaneous excitation of fluctuations with different scale lengths is not allowed. Fluctuation is given by the micro mode in this graph. Further detailed analysis will be presented in a forthcoming article.[26]

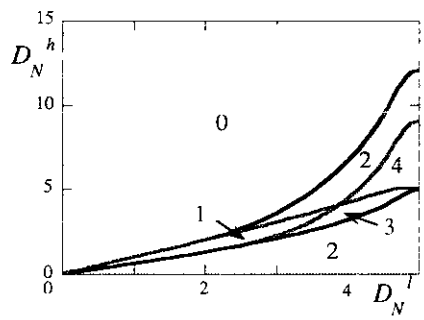

Fig.8 Phase diagram of turbulent state on the plane of normalized parameters $D_N^l = D^l/\sqrt{I_{eff}^{h\leftarrow l}}$ and $D_N^h = D^h/\sqrt{I_{eff}^{h\leftarrow l}}$. D^m is fixed as $D^m = \left(1/5\right)\sqrt{I_{eff}^{h\leftarrow l}}$. Numbers in the diagram denote the possible numbers of branches in which all the three components are simultaneously excited.

Transitions between different branches take place at the boundaries of the diagram if the excitation by the noise is neglected.

VI. SUMMARY

In this article, the statistical theory of plasma turbulence is applied to analyzing the state where fluctuations with different scale lengths coexist. The nonlinear interactions between the micro mode and the semi-micro mode are taken into account. The nonlinear dynamics determines both the fluctuation levels and the cross field turbulent transport for the fixed global parameters . A quenching or suppressing effect is induced by their nonlinear interplay, even if both modes are unstable when analyzed independently. The thermal fluctuation of the scale length of λ_D is assumed to be statistically independent. The hierarchical structure is constructed according to the scale lengths. Transitions in turbulence are found and phase diagrams with cusp type catastrophe are obtained. Dynamics is followed. Statistical properties of the subcritical excitation are discussed. The probability density function (PDF) and transition probability are obtained. Power-laws are obtained in the PDF as well as in the transition probability. Generalization for the case where turbulence is composed of three-classes of modes is also developed. A new catastrophe of turbulent states is obtained.

The result clearly shows that the nonlinear interplay among turbulence modes is essential. An independent analysis of the mode and their suppression are not sufficient for the solution of the problem.

The formulation in this article is easily extended to various cases. One application is the analysis of the nonlocal transport problem, which has been analyzed in conjunction with the transient response problems. The contribution of the long-wave-length mode, which is excited by the statistical noise process of micro-turbulence is discussed in ref.14.

ACKNOWLEDGEMENTS

Authors cordially acknowledge Prof. A. Yoshizawa, Prof. R. Balescu, Prof. A. Fukuyama, Dr. J. A. Krommes and Prof. P. H. Diamond for elucidating comments and useful discussions. They are also grateful to Dr. A. Fujisawa, Dr. Y. Miura, Prof. K. Ida Dr. K.-L. Wong and Prof. F. Wagner for continuous discussions on experimental observations. The work is partially supported by the Grant-in-Aid for Scientific Research of Ministry of Education, Culture, Sports, Science and Technology of Japan, the collaboration program of National Institute for Fusion Science and the collaboration programme of Research Institute for Applied Mechanics of Kyushu University. Two of the authors (SII and KI) acknowledge Research-Award Programme of Alexander von Humboldt-Stiftung (AvH).

REFERENCE

[1] A. Yoshizawa, S.-I. Itoh, K. Itoh, N. Yokoi: Plasma Phys. Control. Fusion **43** R1 (2001).

[2] J. W. Connor: Plasma Phys. Contr. Fusion **30** 619 (1988).

[3] C. W. Horton: Rev. Mod. Phys. **71** 735 (1999).

[4] J. A. Krommes: "Fundamental statistical theories of plasma turbulence in magnetic fields" Phys. Reports in press (2001).

[5] K. Itoh, S.-I. Itoh and A. Fukuyama: *Transport and Structural Formation in Plasmas* (IOP, Bristol, 1999)

[6] S.-I. Itoh, K. Itoh, A. Fukuyama and Y. Miura : *Phys. Rev. Lett.* **67** 2485 (1991).

[7] P. H. Diamond, et al.: Phys. Rev. Lett. **78** 1472 (1997).

[8] A. I. Smolyakov and P. H. Diamond: Phys. Plasmas **6** 4410 (1999).

[9] J. F. Drake, A. Zeiler, D. Biskamp: Phys. Rev. Lett. **75** 4222 (1995).

[10] J .A. Krommes and C.-B. Kim: Phys. Rev. E. **62** 8508 (2000).

[11] J. A. Krommes: Plasma Phys. Contr. Fusion **41** A641 (1999).

[12] S.-I. Itoh and K. Itoh: J. Phys. Soc. Jpn. **68** 1891, 2611 (1999): **69** 408, 3253 (2001) .

[13] S.-I. Itoh and K. Itoh: J. Phys. Soc. Jpn. **69** 427 (2000).

[14] S.-I. Itoh and K. Itoh: Plasma Phys. Contr. Fusion **43** 1055 (2001).

[15] M. Yagi: PhD thesis: *Study of anomalous transport based on drift and resistive i nstabilities in Heliotron/torsatron configuration* (Kyoto University, 1989).

[16] R. H. Kraichnan: J. Fluid Mech. **41** 189 (1970).

[17] T. S. Hahm: "Physics behind transport barrier theory and simulations" presented at 8th IAEA Technical Committee Meeting on H-mode Physics and Transport Barriers Physics (Toki, 2001) and to be published in Plasma Phys. Contr. Fusion **43** (2001)

[18] R. J. Fonck et al.: *Plasma Physics and Contrlled Nuclear Fusion Research 1990* (Washington, IAEA, 1990) Vol.2, p. 53

[19] K.-L. Wong et al.: Phys. Lett. A **236** 33 (1997).

[20] E. Mazzucato et al.: Phys. Rev. Lett. **77** 3145 (1996).

[21] K.-L. Wong, , et al.: Phys. Lett. A **276** 281 (2000).

[22] M. Uchida, A. Fukuyama, K. Itoh, S.-I. Itoh, M. Yagi: J. Plasma Fusion Res. SERIES, **2** 117 (1999)

[23] M. Kawasaki, et al.: "Transition Probability to Turbulent Transport Regime and Its Critical Exponent" presented at 8th IAEA Technical Committee Meeting on H-mode Physics and Transport Barriers Physics (Toki, 2001) and to be published in Plasma Phys. Contr. Fusion **43** (2001)

[24] I. Prigogine: *Introduction to Thermodynamics of Irreversible Processes*, 2nd ed. (Interscience Publishers, New York, 1961).

[25] R. H. Fowler: *Statistical Mechanics* (second ed., Cambridge, 1936) Chap.18.

[26] S.-I. Itoh, A. Kitazawa, et al.: paper in preparation.

Recent Issues of NIFS Series

NIFS-703 S -I Itoh and K Itoh
Statistical Theory and Transition in Multiple-scale-lengths Turbulence in Plasmas
June 2001

NIFS-704 S Toda and K Itoh
Theoretical Study of Structure of Electric Field in Helical Toroidal Plasmas
June 2001

NIFS-705 K Itoh and S-I Itoh
Geometry Changes Transient Transport in Plasmas
June 2001

NIFS-706 M Tanaka and A. Yu. Grosberg
Electrophoresis of Charge Inverted Macroion Complex Molecular Dynamics Study
July 2001

NIFS-707 T-H Watanabe, H Sugama and T Sato
A Nondissipative Simulation Method for the Drift Kinetic Equation
July 2001

NIFS-708 N Ishihara and S Kida
Dynamo Mechanism in a Rotating Spherical Shell: Competition between Magnetic Field and Convection Vortices
July 2001

NIFS-709 LHD Experimental Group
Contributions to 28th European Physical Society Conference on Controlled Fusion and Plasma Physics (Madeira Tecnopolo, Funchal, Portugal, 18-22 June 2001) from LHD Experiment
July 2001

NIFS-710 V Yu Sergeev, R K Janev, M.J Rakovic, S Zou, N Tamura, K.V. Khlopenkov and S Sudo
Optimization of the Visible CXRS Measurements of TESPEL Diagnostics in LHD
Aug. 2001

NIFS-711 M. Bacal, M Nishiura, M. Sasao, M. Wada, M. Hamabe and H. Yamaoka
Effect of Argon Additive in Negative Hydrogen Ion Sources
Aug 2001

NIFS-712 K Saito, R. Kumazawa, T Mutoh, T Seki, T Watari, T. Yamamoto, Y Torii, N Takeuchi C Zhang, Y. Zhao, A Fukuyama, F Shimpo, G. Nomura, M. Yokota, A Kato, M Sasao, M Isobe, A V Krasilnikov, T. Ozaki, M. Osakabe, K Narihara, Y. Nagayama, S Inagaki, K Itoh, T. Ido, S Morita, K Ohkubo, M. Sato, S. Kubo, T. Shimozuma, H Idei, Y. Yoshimura, T. Notake, O Kaneko, Y. Takeiri, Y. Oka, K Tsumori, K. Ikeda, A. Komori, H Yamada, H Funaba, K.Y. Watanabe, S Sakakibara, R. Sakamoto, J. Miyazawa, K Tanaka, B.J Peterson, N Ashikawa, S. Murakami, T Minami, M. Shoji, S Ohdachi, S Yamamoto, H Suzuki, K Kawahata, M Emoto, H. Nakanishi, N. Inoue, N Ohyabu, Y Nakamura, S. Masuzaki, S Muto, K. Sato, T Morisaki, M Yokoyama, T Watanabe, M. Goto, I. Yamada, K. Ida, T. Tokuzawa, N Noda, K. Toi, S. Yamaguchi, K Akaishi, A Sagara, K. Nishimura, K Yamazaki, S. Sudo, Y Hamada, O. Motojima, M Fujiwara
A Study of High-Energy Ions Produced by ICRF Heating in LHD
Sep 2001

NIFS-713 Y Matsumoto, S -I Oikawa and T. Watanabe
Field Line and Particle Orbit Analysis in the Periphery of the Large Helical Device
Sep. 2001

NIFS-714 S. Toda, M. Kawasaki, N. Kasuya, K. Itoh, Y. Takase, A. Furuya, M. Yagi and S -I. Itoh
Contributions to the 8th IAEA Technical Committee Meeting on H-Mode Physics and Transport Barriers (5-7 September 2001, Toki, Japan)
Oct 2001

NIFS-715 A Maluckov, N. Nakajima, M Okamoto, S Murakami and R. Kanno
Statistical Properties of the Particle Radial Diffusion in a Radially Bounded Irregular Magnetic Field
Oct 2001

NIFS-716 Boris V. Kuteev
Kinetic Depletion Model for Pellet Ablation
Nov. 2001

NIFS-717 Boris V Kuteev and Lev D Tsendin
Analytical Model of Neutral Gas Shielding for Hydrogen Pellet Ablation
Nov 2001

NIFS-718 Boris V. Kuteev
Interaction of Cover and Target with Xenon Gas in the IFE-Reaction Chamber
Nov. 2001

NIFS-719 A. Yoshizawa, N. Yokoi, S.-I Itoh and K. Itoh
Mean-Field Theory and Self-Consistent Dynamo Modeling
Dec 2001

NIFS-720 V.N. Tsytovich and K Watanabe
Universal Instability of Dust Ion-Sound Waves and Dust-Acoustic Waves
Jan. 2002

NIFS-721 V N. Tsytovich
Collective Plasma Corrections to Thermonuclear Reactions Rates in Dense Plasmas
Jan 2002

NIFS-722 S. Toda and K Itoh
Phase Diagram of Structure of Radial Electric Field in Helical Plasmas
Jan. 2002

NIFS-723 V.D. Pustovitov
Ideal and Conventional Feedback Systems for RWM Suppression
Jan. 2002

NIFS-724 T. Watanabe and H Hojo
The Marginally Stable Pressure Profile and a Possibility toward High Beta Plasma Confinement in LHD
Feb 2002

NIFS-725 S -I Itoh, K. Itoh, M Yagi, M Kawasaki and A Kitazawa
Transition in Multiple-scale lengths Turbulence in Plasmas
Feb 2002